typeset using JPSJ.sty <ver.1.0b>

Two-Dimensional σ-Hole Systems in Boron Layers: A First-Principles Study on $Mg_{1-x}Na_xB_2$ and $Mg_{1-x}Al_xB_2$

Shugo SUZUKI, Shin'ichi HIGAI[1] and Kenji NAKAO

Institute of Materials Science, University of Tsukuba, Tsukuba 305-8573
[1] *National Research Institute for Metals, 1-2-1 Sengen, Tsukuba 305-0047*
(Received February 8, 2001)

We study two-dimensional σ-hole systems in boron layers by calculating the electronic structures of $Mg_{1-x}Na_xB_2$ and $Mg_{1-x}Al_xB_2$. In $Mg_{1-x}Na_xB_2$, it is found that the concentration of σ holes is approximately described by $(0.8 + 0.8x) \times 10^{22}$ cm^{-3} and the largest attainable concentration is about 1.6×10^{22} cm^{-3} in NaB_2. In $Mg_{1-x}Al_xB_2$, on the other hand, it is found that the concentration of σ holes is approximately described by $(0.8 - 1.4x) \times 10^{22}$ cm^{-3} and σ holes disappear at x of about 0.6. These relationships can be used for experimental studies on σ-hole systems in these materials.

KEYWORDS: MgB_2, NaB_2, AlB_2, σ holes, two dimension, hole concentration

Recently, Nagamatsu et al. have discovered that magnesium diboride, MgB_2, is a superconductor with a high transition temperature, T_c, of 39 K.[1)] Extensive studies have now started both experimentally and theoretically. In particular, since MgB_2 can be regarded as a starting material for undiscovered high-T_c superconductors, it is important to search for various materials derived from MgB_2.

The structure of MgB_2 consists of layers of triangular lattices of Mg atoms and layers of honeycomb lattices of B atoms.[2)] This structure is basically the same as that of the alkali-metal binary graphite intercalation compounds (GIC).[3)] Since Mg and B are light elements, where the s and p atomic orbitals play dominant roles, the electronic structure of MgB_2[4)] is also very similar to those of GIC.[5)] In spite of these similarities, there are no GIC superconductors developed with such a high T_c; the highest T_c of alkali-metal GIC is only about 0.15 K for C_8K.[6)]

One significant difference between MgB_2 and GIC is the existence of the σ holes at the center of the Brillouin zone,[4)] which are derived from the $2p_x$ and $2p_y$ atomic orbitals of B. Since the σ bands in graphite layers are energetically very deep, the generation of σ holes is extremely difficult in GIC. Furthermore, it is interesting to note that holes in boron layers will show characteristics of two-dimensional (2D) systems. As revealed thus far, 2D systems can provide a rich variety of physics and possibilities of applications. It is thus important for understanding the properties of MgB_2 and its derivatives to study the electronic structures of the σ-hole systems in boron layers.

In this Letter, we study the 2D σ-hole systems in $Mg_{1-x}Na_xB_2$ and $Mg_{1-x}Al_xB_2$ at x=0, 1/3, 2/3, and 1 by calculating the electronic structures of these materials based on the density functional theory. The main results of the present study are as follows. In $Mg_{1-x}Na_xB_2$, since Na is a monovalent metal, the concentration of σ holes is increased with increasing x, approximately described by $(0.8+0.8x)\times10^{22}\mathrm{cm}^{-3}$. In $Mg_{1-x}Al_xB_2$, on the contrary, since Al is a trivalent metal, the concentration of σ holes is reduced with increasing x, approximately described by $(0.8-1.4x)\times10^{22}\mathrm{cm}^{-3}$. In the latter case, the σ holes disappear at x of about 0.6. These results can be used for experimental studies on σ-hole systems in these materials.

In the present study, we carry out first-principles calculations based on the density functional theory with the local density approximation[7–10] by considering all electrons. To confirm the reliability of the results, the Kohn-Sham equations are solved using both the mixed-basis method and the linear-combination-of-atomic-orbital (LCAO) method.[11] In this paper, we present the results obtained using the mixed-basis method although the same results can also be obtained using the LCAO method. The cut-off energy used for plane waves is 50 eV and the atomic orbitals employed as localized orbitals are given in Table I. We use not only the atomic orbitals of neutral atoms but also those of charged atoms to increase the variational flexibility. The number of used k points in the full Brillouin zone is 52 for the structure optimization of NaB_2 and 185 for the electronic structure calculations of NaB_2, MgB_2, and AlB_2. Moreover, that used in the calculations of $Mg_{1-x}Na_xB_2$ and $Mg_{1-x}Al_xB_2$ is 104.

We first calculate the electronic structures of NaB_2, MgB_2, and AlB_2. The calculations are performed using the experimental lattice constants of MgB_2 and AlB_2; a = 3.084 Å and c = 3.522 Å are used for MgB_2 and a = 3.009 Å and c = 3.262 Å are used for AlB_2. On the other hand, since NaB_2 is a hypothetical material at present, it is necessary to optimize the lattice constants of this material. The resultant constants a and c are 3.02 Å and 4.19 Å, respectively, and are used for NaB_2. To confirm the reliability of this result, we also optimize the structure of MgB_2 and find that the errors for a and c are -2 % and $+0.5$ %, respectively. We thus believe that the result for NaB_2 is also reliable with the same accuracy. The lattice constants c of these materials can be understood by considering the fact that the ionic radii of Na^+, Mg^{2+}, and Al^{3+} are 0.97 Å, 0.65 Å, and 0.50 Å, respectively.

In Figs. 1(a), 1(b), and 1(c), the calculated electronic structures of NaB_2, MgB_2, and AlB_2 are shown, respectively. The dotted lines in the figures indicate the Fermi level. The most impressive point is the position of the top of the σ bands derived from the $2p_x$ and $2p_y$ atomic orbitals of B. In NaB_2 and MgB_2, the top of the σ bands is above the Fermi level, and accordingly, there exist σ holes in these materials. This is in strong contrast to the fact that there are no σ holes in GIC. Since Na is a monovalent metal while Mg is a divalent metal, the concentration of σ holes is higher in NaB_2 than in MgB_2. Thus, the concentration of the σ holes can be increased when we increase

x in $Mg_{1-x}Na_xB_2$. On the contrary, in AlB_2, the top of the σ bands is below the Fermi level and accordingly there are no σ holes in this material. Thus, the concentration of σ holes is reduced when we increase x in $Mg_{1-x}Al_xB_2$, and eventually they disappear at a certain value of x.

Furthermore, since the dispersion of the top of the σ bands of all the materials is very small along the Γ-A direction, the σ holes can exhibit characteristics of 2D systems such as large fluctuation. This is in strong contrast to the three-dimensionality of other carriers in these materials. In all the materials studied, there exist three-dimensional (3D) π electrons and/or holes. Moreover, in AlB_2, there exist a small number of 3D electrons in the nearly free electron state at the Γ point, which is derived from the hybridization between the $3s$ atomic orbitals of Al and the interlayer state of boron layers; this is very similar to the situation in C_8K, where the nearly free electrons also exist at the Γ point.[12] It should be noted that, in GIC, there exist π electrons and/or holes and also nearly free electrons and not σ holes.

Next, we study the electronic structures of $Mg_{1-x}Na_xB_2$ and $Mg_{1-x}Al_xB_2$ at x=0, 1/3, 2/3, and 1. In the calculations, we assume an in-plane $(\sqrt{3} \times \sqrt{3})$ structure, as shown in Fig. 2. This structure is simple because the threefold rotation axis also exists as in the (1×1) original structure, and thus, the same Brillouin zone can be used. We also assume that the lattice constants of these materials can be obtained by linearly interpolating between the lattice constants of MgB_2 and NaB_2 or AlB_2. As an example, we show the result for $Mg_{2/3}Na_{1/3}B_2$ in Fig. 3. The obtained electronic structure can be understood by considering the folding of the original band structures shown in Fig. 1. The σ bands are easily identified to be the bands with small dispersion along the Γ-A direction immediately above the Fermi level.

In Fig. 4, we show the top of the σ bands in $Mg_{1-x}Na_xB_2$ and $Mg_{1-x}Al_xB_2$ as a function of x. The dotted line in the figure indicates the Fermi level. It is found that the dependence is monotonic and the largest attainable value is 1.8 eV for NaB_2. We also find that, in $Mg_{1-x}Al_xB_2$, the top of the σ bands is below the Fermi level for x larger than about 0.6, that is, the σ holes disappear for such x. The dependence on x for the entire region from NaB_2 to AlB_2 via MgB_2 shown in Fig. 4 cannot be fitted with a single straight line. It is necessary to fit the result with a curve or, at least, with two straight lines, one for $Mg_{1-x}Na_xB_2$ and the other for $Mg_{1-x}Al_xB_2$. If we select the latter choice, the result can be fitted with

$$\varepsilon_{\rm top} = 0.90 + 0.91x \text{ eV} \tag{0.1}$$

for $Mg_{1-x}Na_xB_2$ and with

$$\varepsilon_{\rm top} = 0.90 - 1.57x \text{ eV} \tag{0.2}$$

for $Mg_{1-x}Al_xB_2$. Here, we ignore the point for AlB_2 in obtaining the above formulae because some quantities, including the top of the σ bands and the cohesive energy as shown below, are not on

the same straight line as the other $Mg_{1-x}Al_xB_2$; this can be ascribed to the existence of the nearly free electrons in AlB_2 which do not exist in the other $Mg_{1-x}Al_xB_2$ calculated in the present study.

In Fig. 5, we show the cohesive energy of $Mg_{1-x}Na_xB_2$ and $Mg_{1-x}Al_xB_2$ as a function of x. It is found that the most stable material is AlB_2 and the least stable one is NaB_2. The dependence on x for the entire region from NaB_2 to AlB_2 via MgB_2 can be described by a single straight line if we ignore the point for AlB_2 because the cohesive energy may be affected by the existence of the nearly free electrons as mentioned above. The result can be fitted with

$$E_{\rm c} = 5.59 - 0.62x \text{ eV/atom} \tag{0.3}$$

for $Mg_{1-x}Na_xB_2$ and with

$$E_{\rm c} = 5.59 + 0.62x \text{ eV/atom} \tag{0.4}$$

for $Mg_{1-x}Al_xB_2$. Although NaB_2 is a hypothetical material at present, we believe that this material can be synthesized under some appropriate conditions because the cohesive energy of NaB_2, about 5 eV/atom, is not very small; it is almost the same as that of the bulk Si.

Next, we study the dependence of the concentration of σ holes on x by assuming a constant density of states for the upper region of the σ bands. This assumption is good as long as two conditions are satisfied; one is that the dispersion along the Γ-A direction is very small and the other is that the deviation from the in-plane free-electron-like dispersion is negligible. Since both conditions are satisfied as shown in Fig. 1, we derive the formulae which give the concentration of σ holes for a given x. First, it is necessary to fit the in-plane free-electron-like dispersion using effective masses for heavy and light holes. As a result, we find that the effective mass for heavy holes is $0.5m_{\rm e}$ and that for light holes is $0.3m_{\rm e}$, where $m_{\rm e}$ is the mass of free electrons. Next, by combining these results with those shown in Fig. 4, the following formulae are derived to determine the concentration of the σ holes:

$$n_{\rm h} = (0.8 + 0.8x) \times 10^{22} \text{ cm}^{-3} \tag{0.5}$$

or

$$n_{\rm h} = 0.12 + 0.12x \text{ /B atom} \tag{0.6}$$

for $Mg_{1-x}Na_xB_2$ and

$$n_{\rm h} = (0.8 - 1.4x) \times 10^{22} \text{ cm}^{-3} \tag{0.7}$$

or

$$n_{\rm h} = 0.12 - 0.21x \text{ /B atom} \tag{0.8}$$

for $Mg_{1-x}Al_xB_2$. Thus, in $Mg_{1-x}Na_xB_2$, the largest attainable concentration of σ holes is about 1.6×10^{22} cm^{-3} in NaB_2. In $Mg_{1-x}Al_xB_2$, on the other hand, σ holes disappear at x of about 0.6.

Here, we discuss the possibility of LiB_2 as a candidate for increasing the concentration of σ holes. Although one may expect that LiB_2 is the most plausible candidate because of the almost same ionic radius of Li^+, 0.68 Å, as that of Mg^{2+}, this may not be the case. We have found that the structure optimization of LiB_2 results in strong contraction of c, which is found to be less than 3 Å. The result strongly conflicts with a simple expectation that the lattice constant c of LiB_2 should be about 3.6 Å if we estimate it by considering the ionic radius of Li^+. To elucidate the stable structure of LiB_2, our study on this is now in progress. In spite of this result, one can still expect that $Mg_{1-x}Li_xB_2$ for sufficiently small x can be synthesized because the introduction of sufficiently small Li cannot affect the lattice constant c very strongly.

We next discuss the difference between MgB_2 and other metal diborides such as transition-metal (TM) diborides[13] and noble-metal diborides, AgB_2 and AuB_2. The most important point is the absence of d atomic orbitals in MgB_2 in contrast to the existence of d atomic orbitals in other metal diborides. In particular, since the d atomic orbitals in TM are partly filled, they form strong covalent bonding with σ bonds of boron layers. This can destroy a 2D σ-hole system in boron layers; we have calculated the electronic structures of some TM diborides and have found that the σ bands of boron layers are strongly affected by the covalent bonding with d atomic orbitals of TM. On the other hand, AgB_2 and AuB_2 can be candidates for materials similar to MgB_2. The reason for this is that the σ holes may survive in these materials because d atomic orbitals in these materials should be sufficiently lower than the Fermi level, and thus, the hybridization between the d atomic orbitals and the σ bands may occur at a lower-energy region.

We finally discuss the possible relationship between the superconductivity in MgB_2 and the 2D σ-hole systems in boron layers. If the superconductivity in $Mg_{1-x}Al_xB_2$ disappears at x of about 0.6, it should be caused by the σ-hole systems. In addition, there are no TM diborides with T_c as high as that of MgB_2; this may be due to the fact that they have no σ holes. If this is the case, both the electron-phonon interaction and the electron correlation may be the likely origins of the superconductivity. Since σ bonds, particularly those of B, C, N, and O, are very strong, the interaction between the σ holes and the in-plane σ-bond vibration is also expected to be very strong. Furthermore, this electron-phonon coupling can result in a superconductivity of high T_c because the frequency of the σ-bond vibration is of the order of 0.2 eV. On the other hand, the electron correlation in the σ holes appears also important for the properties of the σ-hole system in MgB_2 because the wave function of the σ holes is localized to a considerable degree.

Acknowledgements

We would like to thank J. Akimitsu, T. Arima, Y. Iwasa, and H. Tsunetsugu for useful discussions.

References

1) J. Nagamatsu, N. Nakagawa, T. Muranaka, Y. Zenitani and J. Akimitsu: Nature **410** (2001) 63.
2) V. Russell, R. Hirst, F. A. Kanda and A. J. King: Acta. Cryst. **6** (1953) 870.
3) M. S. Dresselhaus and G. Dresselhaus: Adv. Phys. **30** (1981) 139.
4) D. R. Armstrong and P. G. Perkins: J. Chem. Soc., Faraday Trans. 2 **75** (1979) 12.
5) N. A. W. Holzwarth: *Graphite Intercalation Compounds II*, eds. H. Zabel and S. A. Solin (Springer Verlag, Berlin, 1992) p. 7.
6) S. Tanuma: *Graphite Intercalation Compounds II*, eds. H. Zabel and S. A. Solin (Springer Verlag, Berlin, 1992) p. 163.
7) P. Hohenberg and W. Kohn: Phys. Rev. **136** (1964) B864.
8) W. Kohn and L. J. Sham: Phys. Rev. **140** (1965) A1133.
9) J. P. Perdew and A. Zunger: Phys. Rev. B **23** (1981) 5048.
10) D. M. Ceperley and B. J. Alder: Phys. Rev. Lett. **45** (1980) 566.
11) S. Suzuki and K. Nakao: J. Phys. Soc. Jpn. **69** (2000) 532.
12) S. Amamiya, S. Higai, S. Suzuki and K. Nakao: Mol. Cryst. Liq. Cryst. **340** (2000) 53.
13) P. Vajeeston, P. Ravindran, C. Ravi and R. Asokamani: Phys. Rev. B **63** (2001) 45115.

Figure Captions

Fig. 1. Band structures of (a) NaB_2, (b) MgB_2, and (c) AlB_2. The dotted lines indicate the Fermi level.

Fig. 2. In-plane ($\sqrt{3} \times \sqrt{3}$) structure (dashed lines) used in the electronic structure calculations of $Mg_{1-x}M_xB_2$ (M=Na or Al, x=0, 1/3, 2/3, and 1) and original (1×1) structure (dotted lines). Small closed circles represent B atoms and large circles represent the other atoms. For x=0, all the large circles are Mg atoms. For x=1/3, open and hatched circles are Mg and M atoms, respectively. For x=2/3, open and hatched circles are M and Mg, respectively. For x=1, all the large circles are M atoms.

Fig. 3. Band structure of $Mg_{2/3}Na_{1/3}B_2$. The dotted lines indicate the Fermi level.

Fig. 4. Top of the σ bands as a function of x. The horizontal axis is from NaB_2 to AlB_2 via MgB_2. The dotted line indicates the Fermi level. The solid line fits the four points for $Mg_{1-x}Na_xB_2$. The dotted-dashed line fits the three points for $Mg_{1-x}Al_xB_2$, ignoring the point for AlB_2.

Fig. 5. Cohesive energy as a function of x. The horizontal axis is from NaB_2 to AlB_2 via MgB_2. The solid line fits the six points for $Mg_{1-x}Na_xB_2$ and $Mg_{1-x}Al_xB_2$, ignoring the point for AlB_2.

Table I. Atomic orbitals used for mixed-basis calculations.

Atom	Atomic orbitals (atomic charge)
B	$1s$,$2s$,$2p$(neutral)
Na	$1s$,$2s$,$2p$,$3s$(neutral)
Mg	$1s$,$2s$,$2p$,$3s$(neutral); $3p$(1+); $3d$(2+)
Al	$1s$,$2s$,$2p$,$3s$,$3p$(neutral); $3d$(2+)

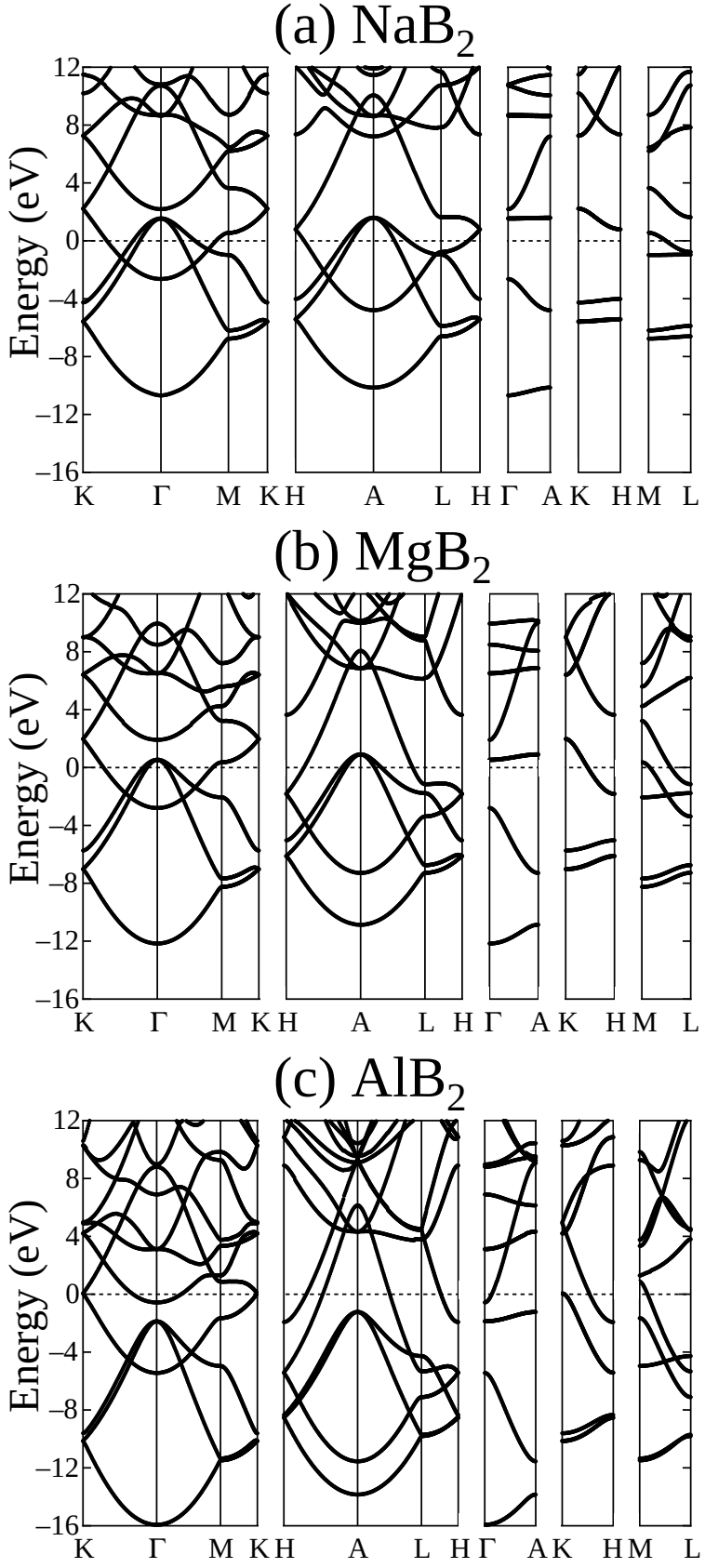

Fig. 1

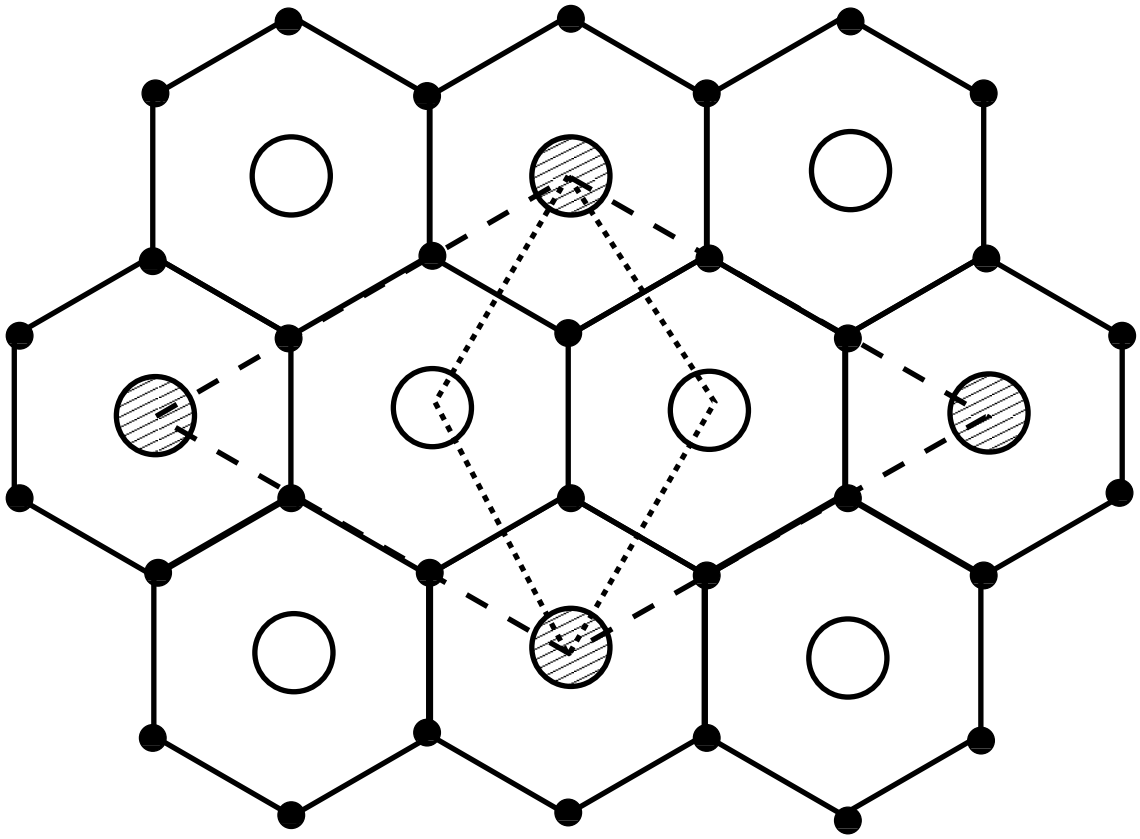

Fig. 2

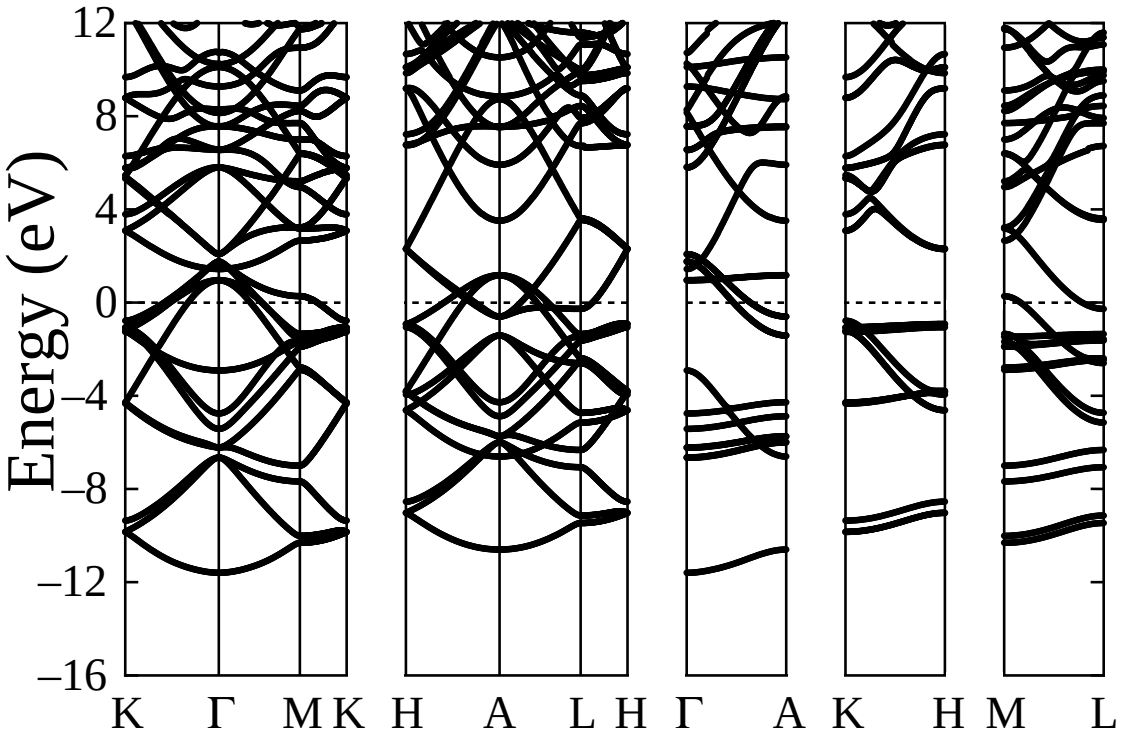

Fig. 3

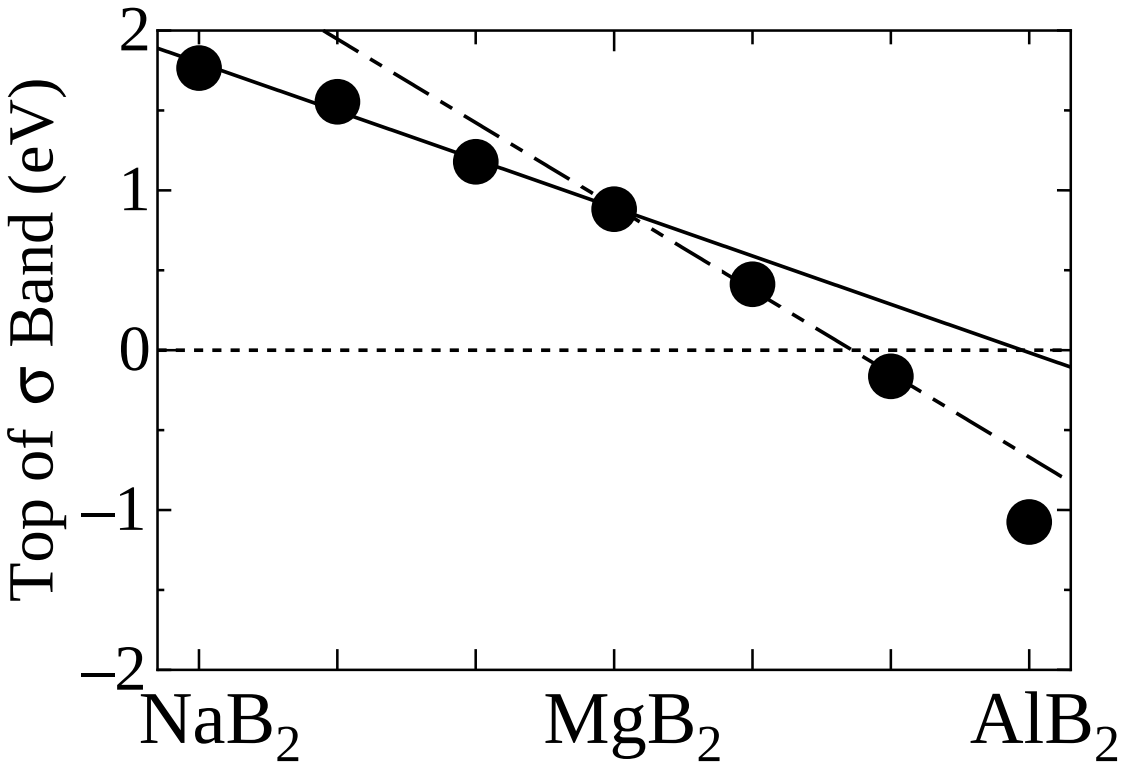

Fig. 4

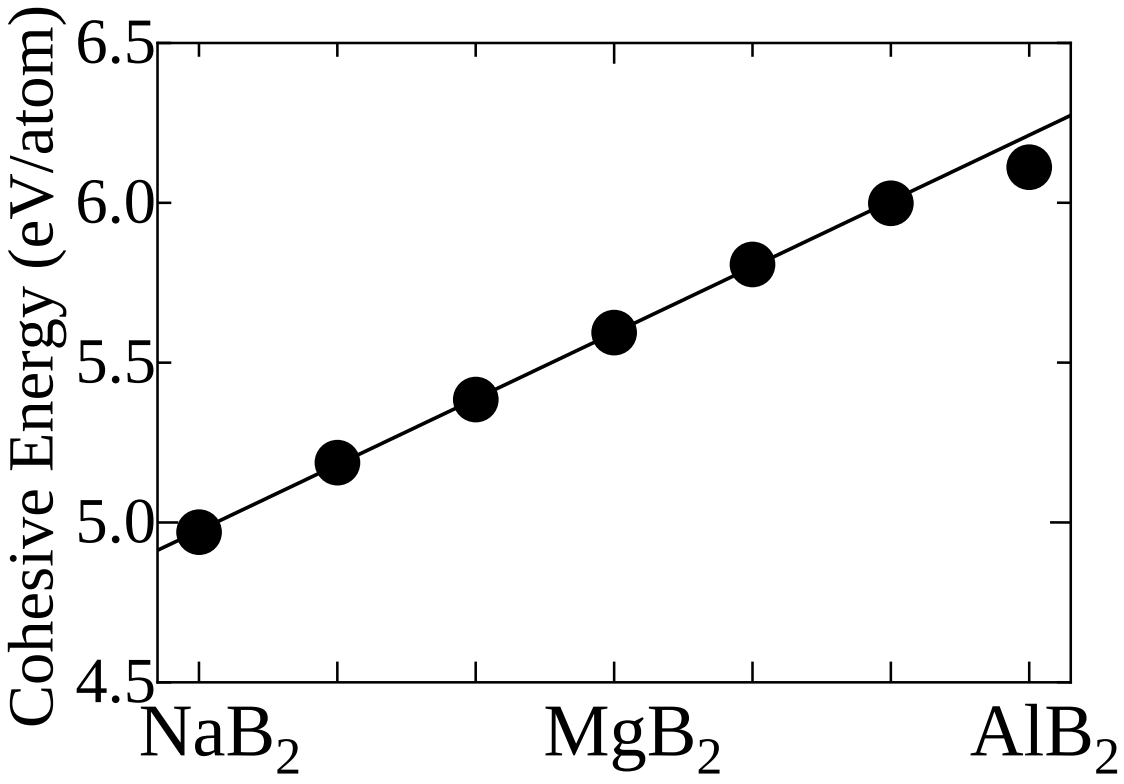

Fig. 5